Science of the Total Environment 676 (2019) 613–626

Contents lists available at ScienceDirect

Science of the Total Environment

journal homepage: www.elsevier.com/locate/scitotenv

Identifying climate change impacts on water resources in Xinjiang, China

Min Luo [a,b,c,d,e,i], Tie Liu [a,i,*], Fanhao Meng [f], Yongchao Duan [a,b,c,d,e], Anming Bao [a], Wei Xing [a], Xianwei Feng [g], Philippe De Maeyer [b,d,e], Amaury Frankl [b,h]

[a] State Key Laboratory of Desert and Oasis Ecology, Xinjiang Institute of Ecology and Geography, Chinese Academy of Sciences, Urumqi 830011, China
[b] Department of Geography, Ghent University, Gent 9000, Belgium
[c] University of Chinese Academy of Science, Beijing 100049, China
[d] Sino-Belgian Joint Laboratory of Geo-information, Urumqi, China
[e] Sino-Belgian Joint Laboratory of Geo-information, Gent, Belgium
[f] Inner Mongolia Normal University, Hohhot 010022, China
[g] Shanghai Branch of Chinese Academy of Science, Shanghai 200031, China
[h] Research Foundation Flanders (FWO), 1000 Brussels, Belgium
[i] CAS Research Center for Ecology and Environment of Central Asia, Urumqi 830011, China

HIGHLIGHTS

- The elevation, area and aspect of catchments affect the extent of impacts.
- The impact of warming on discharge will change from positive into negative.
- The overall increases in water resources in Xinjiang, China are not sustainable.

GRAPHICAL ABSTRACT

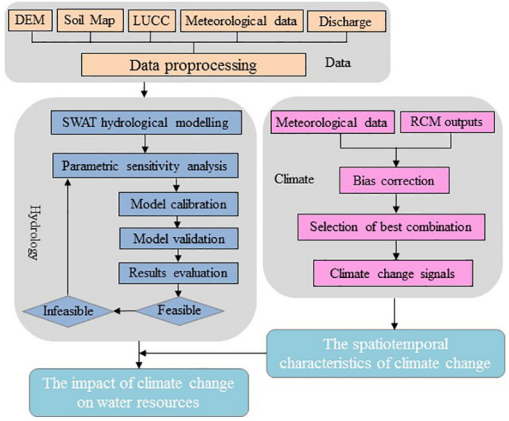

ARTICLE INFO

Article history:
Received 29 November 2018
Received in revised form 17 April 2019
Accepted 19 April 2019
Available online 24 April 2019

Editor: Ralf Ludwig

Keywords:
SWAT
RCP

ABSTRACT

Water resources have an important role in maintaining ecological fuctions and sustaining social and economic development. This is especially true in arid and semi-arid areas, where climate change has a large impact on water resources, such as in Xinjiang, China. Using a combination of precipitation and temperature bias correction methods, we analyzed projected changes in different hydrological components in nine high-alpine catchments distributed in Xinjiang using the Soil and Water Assessment Tool (SWAT). The impacts of elevation, area and aspect of the catchments were analyzed. The results suggested an overall warming and wetting trend for all nine catchments in the near future, with the exception of summer precipitation decreasing in some catchments. The total runoff discharge, evapotranspiration and snow/ice melting will generally increase. Warming temperature plays a more important role in the changes of each hydrological component than increasing precipitation. However, northern Xinjiang was more sensitive to

* Corresponding author.
E-mail address: liutie@ms.xjb.ac.cn (T. Liu).

https://doi.org/10.1016/j.scitotenv.2019.04.297

Climate change
Water resources
Catchment

predicted precipitation changes than southern Xinjiang. These results also indicate that the overall increases in water resources are not sustainable, and the impacts of climate change are associated with the elevation, area and slope aspect of the catchments.

1. Introduction

Global climate change and its impact on water resources have received increasingly attention from societies across the world due to the substantial environmental and the economic implications (Jasper et al., 2004; Zhang et al., 2008). The Chinese Xinjiang Uygur Autonomous Region (hereafter Xinjiang) is a (semi-)arid region in Central Asia. In Xinjiang, high-alpine environments are the source areas for rivers that provide water for agricultural, industrial and domestic purposes (Fang et al., 2015a; Liu et al., 2011). However, the provision of water by the high-alpine rivers is expected to be altered substantially because of climate change (Bradley et al., 2006). Consequently, water resource management and allocation, which already create conflicts due to water shortages and highly uneven spatial distribution, are expected to become more problematic in the near future (Chen et al., 2011).

The General Circulation Models (GCMs) developed in the fifth phase of the Coupled Model Intercomparison Project (CMIP5) of the Intergovernmental Panel on Climate Change (IPCC) are the most advanced tools currently available for both present and future climate change projections (Wilby and Wigley, 1997). However, due to their coarse resolution (ca. 150–300 km), they do not allow the study of coupled climate-hydrological systems at a regional scale (Lespinas et al., 2014). Therefore, GCMs need to be downscaled to finer resolutions (often 10–50 km), which results in Regional Climate Models (RCMs) at local or regional scales (Yang et al., 2010). Although the RCMs perform better in reflecting local climates, errors related to their GCM-origin remain significant (Chen et al., 2013b; Durman et al., 2001). For example, RCM-simulated precipitation outputs generally overestimate low-intensity rainfall and underestimate high-intensity rainfall (Teutschbein and Seibert, 2012). Furthermore, as errors will transfer to uncertainties in other model applications, the direct use of RCM-outputs in hydrological impact studies remains challenging (Casanueva et al., 2016; Fowler et al., 2007).

Therefore, preprocessing (via bias correction) of RCM-outputs (mainly precipitation and temperature) is important. Several bias correction techniques have been developed in the last decades (Teutschbein and Seibert, 2012): Linear Scaling (LS), Local Intensity Scaling (LOCI), Daily Bias Correction (DBC), Daily Translation (DT), Power Transformation (PT), Distribution Mapping (DM), Variance Scaling (VARI) and Empirical Quantile Mapping (EQM). Some researchers have evaluated the performances of these methods in different regions (Fang et al., 2015a; Piani et al., 2010; Teutschbein and Seibert, 2012). Chen et al. (2013a) compared the performances of six bias correction methods to correct precipitation for ten catchments in North America. Their results show that improving the RCM-simulated precipitation is possible, but the performance of hydrological modelling depends on the geographic location of catchments and the bias correction methods used. Sunyer et al. (2015) applied bias correction methods to project heavy precipitation in different catchments across Europe and used the outputs to project river flow (Hundecha et al., 2016). A systematic difference of the projections was observed from different methods which was dependent on the flood regime. Teutschbein and Seibert (2012) evaluated six bias correction methods (LS, LOCI, PT, VARI, DM, Delta) in five catchments in Sweden. Technically demanding approaches, such as PT and DM methods performed better for discharge simulations.

The hydrological model Soil and Water Assessment Tool (SWAT) (Arnold et al., 1998) was developed by the United States Department of Agriculture, Agricultural Research Service (USDA-ARS). It has been used to predict discharge in a multitude of catchments globally (Abbaspour et al., 2007; Baker and Miller, 2013; Grusson et al., 2015). It was also successfully used to assess climate change impacts on water resources for several catchments in Xinjiang, such as the Kaidu Catchment (Ba et al., 2018; Fang et al., 2015b), Hotan Catchment (Luo et al., 2017), Yarkant Catchment (Liu et al., 2016; Liu et al., 2017) and Urumqi Catchment (Zhang et al., 2016). However, most studies only focused on specific locations and had a limited spatial extent. Additionally, the impacts of differences in elevation, location, latitude and area, have not been considered thus far to the best of our knowledge.

Here, the combination of EQM-corrected precipitation and VARI-corrected temperature was used to assess the climate change impacts in nine catchments across Xinjiang using SWAT, representing differences in location, elevation and area size. The objective of this study is to understand the impact of climate change on water resources in Xinjiang.

2. Study area and used data

2.1. Study area

Xinjiang is situated in the arid and semi-arid part of Central Asia (Li et al., 2011; Zhang et al., 2015), with mountainous and plain areas accounting for 51.4% and 48.6%, respectively, of the total area (Du et al., 2015). The three main mountain ranges, from north to south, are the Altay (ALT) Mountains, Tianshan (TSH) Mountains and Karakoram (KKM) Mountains (Luo et al., 2018a). These high-elevation areas form the sources of numerous rivers. For this study we selected nine catchments across Xinjiang: Haba (HB), Buerjin (BEJ), Sikeshu (SKS), Santun (ST), Baiyang (BY), Tailan (TL), Kuche (KC), Yeerqiang (YEQ) and Hetian (HT) (Fig. 1). The areas of these catchments vary between 163.2 and 47,313.6 km^2, representing small to large catchments in Xinjiang (Table 1). The annual precipitation ranges from 191.7 and 596.2 mm, with a south-north increasing pattern. Because of the high elevations of the source areas, the catchments have mixed water supplies, mainly from snow and glacier melt and rainfall (Wang and Cheng, 2000).

2.2. Meteorological and river discharge data

Observed daily precipitation, maximum and minimum temperatures, wind speed, relative humidity, and RCM-simulated daily precipitation, maximum and minimum temperatures were used for this study. The observed meteorological data (2008–2011) for the nine selected catchments were obtained from the China Meteorological Data Sharing Service System (http://data.cma.cn/). The daily discharge data (2010−2011) were provided by the Hydrology Bureau of Xinjiang Uygur Autonomous Region. The RCM-simulated meteorological datasets of HadGEM3-RA, SUN-MM5 and RegCM4 (http://www.cordex.org/domains/region-7-east-asia/) were derived from the Coordinated Regional Climate Downscaling Experiment (CORDEX) for the east Asian domain (Giorgi and Gutowski Jr, 2015; Zou et al., 2016). The datasets from CORDEX have been used by many researchers (Dosio et al., 2015; Jacob et al., 2014; Pinto et al., 2018) and show successful applications for Xinjiang (Ba et al., 2018; Luo et al., 2018b). These RCM outputs have a spatial resolution of 50 km. They were corrected with the observed data for the period from 1965 to 2004. Then, the corrected parameters were applied to project the future climate for the period

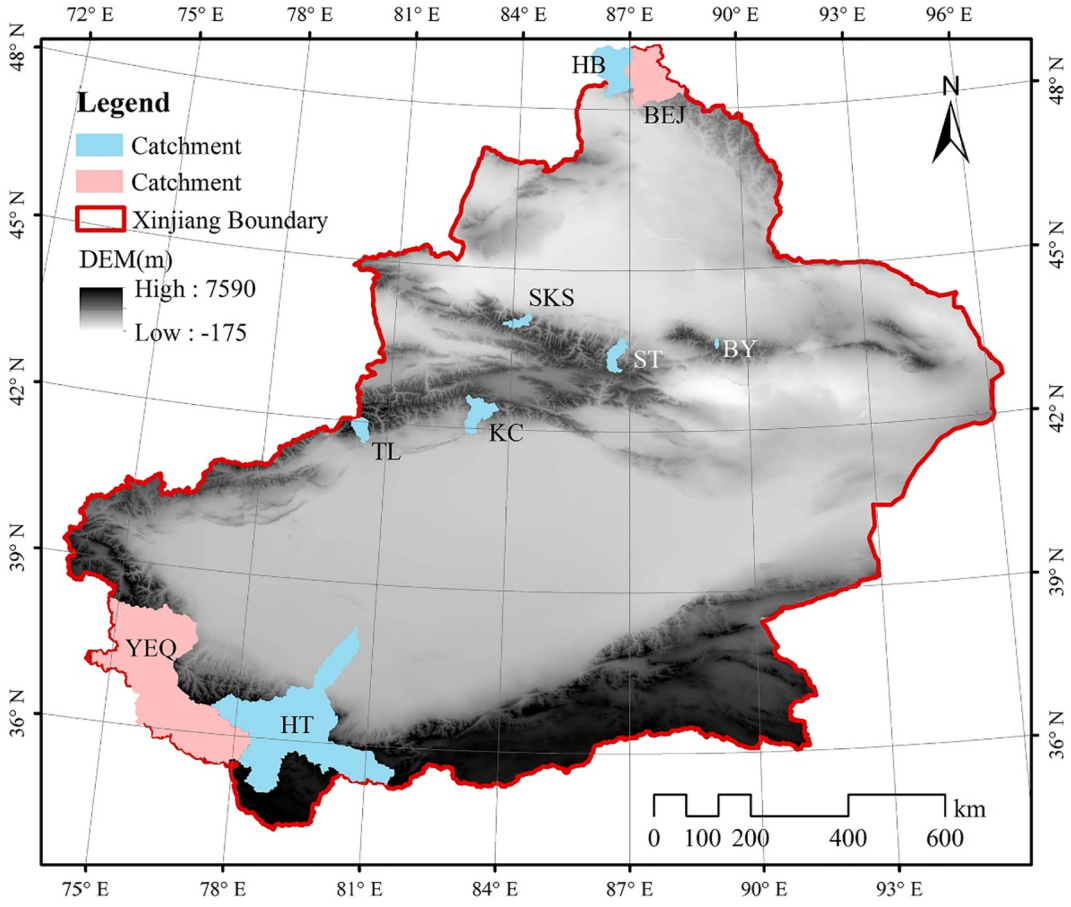

Fig. 1. The location of the nine selected catchments in the Xinjiang Uygur Autonomous Region, China.

2021–2060. The future Representative Concentration Pathway (RCP) emission scenarios, RCP 4.5 and RCP 8.5, representing the respective medium and high emission scenarios, were considered for this study.

3. Methodology

3.1. Hydrological simulation

The SWAT model is a semi-distributed model that requires the following daily meteorological data: precipitation, maximum and minimum temperatures, wind speed, relative humidity and solar radiation. A Digital Elevation Model (DEM), land use/cover map and soil map are also required. Available runoff discharge time series were used to calibrate and validate the model. In this study, the hydrological processes of the nine selected catchments were simulated by using the SWAT model. The meteorological data from the time period of 2008–2009 were used for the model warm-up. The performances of the hydrological model in these catchments were evaluated against the daily discharges as shown in Fig. 2. The calibration and validation of the SWAT model were based on the daily discharge values of 2010 and 2011, respectively. The performance of the modelling results was evaluated by the goodness-of-fit test (R^2) and the Nash–Sutcliffe efficiency coefficient (NSE), defined as follows:

$$R^2 = \frac{\sum_{i=1}^{n}\left(Q_{si}-\overline{Q}_s\right)\left(Q_{oi}-\overline{Q}_o\right)}{\sqrt{\sum_{i=1}^{n}\left(Q_{si}-\overline{Q}_s\right)^2\sum_{i=1}^{n}\left(Q_{oi}-\overline{Q}_o\right)^2}};\ 0\le R^2\le 1, \quad (1)$$

$$NSE = 1-\frac{\sum_{i=1}^{n}(Q_{oi}-Q_{si})^2}{\sum_{i=1}^{n}\left(Q_{oi}-\overline{Q}_o\right)^2};\ -\infty\le NS\le 1, \quad (2)$$

Table 1
Description of the nine selected catchments in Xinjiang (statistics calculated over 2010–2011).

Location	Name	Area (km^2)	Precipitation ($mm\ yr^{-1}$)	Snow fall ($mm\ yr^{-1}$)	Melting water ($mm\ yr^{-1}$)	ET ($mm\ yr^{-1}$)	Elevation (m)
ALT	HB	5867.6	585.8	397.7	356.7	310.3	1821.2
ALT	BEJ	8500.0	571.5	413.8	432.2	110.5	2173.2
KKM	YEQ	47,313.6	301.9	225.3	104.9	72.1	4420.3
KKM	HT	42,873.9	191.7	160.1	163.7	42.8	4173.1
NTSH	SKS	942.8	586.5	493.1	257.9	122.4	3029.8
NTSH	ST	1709.0	334.0	170.6	80.7	206.7	2634.5
NTSH	BY	163.2	595.9	489.4	340.5	170.3	2702.6
STSH	TL	1370.9	596.2	149.8	130.0	139.5	3676.4
STSH	KC	2950.3	253.8	125.7	103.1	88.2	2564.5

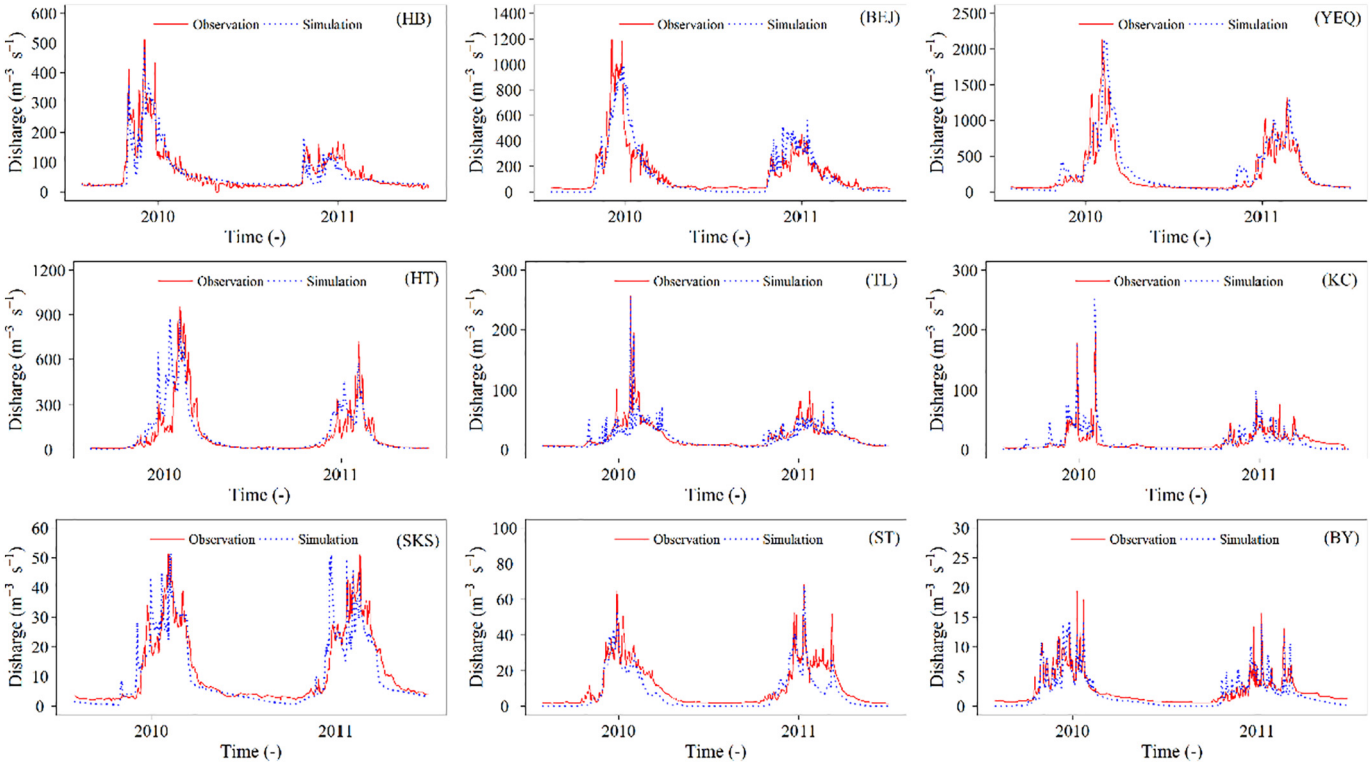

Fig. 2. A comparison of the observed and simulated daily discharge for the nine selected river catchments.

where Q_{si} and Q_{oi} are the simulated and observed discharges, respectively, with $\overline{Q}_s$ and $\overline{Q}_o$ corresponding to their average values.

3.2. Bias correction of RCM derived precipitation and temperature

In a previous study, seven bias correction methods for precipitation and five methods for temperature were selected to correct the raw RCM–outputs for the Kaidu Catchment (Luo et al., 2018b). The precipitation correction methods included LS, LOCI, DBC, DT, PT, DM and EQM, while LS, DT, VARI, DM and EQM were used to correct temperature. Thirty-five possible combinations of corrected precipitation and temperature were applied to drive the SWAT model for daily discharge simulation (Luo et al., 2018b). Based on the performance of the average daily discharge simulation, the combination of EQM-corrected precipitation and VARI-corrected temperature performed best compared to other combinations. Further, both methods show a consistent performance in different catchments (Chen et al., 2013a; Fang et al., 2015a). Therefore, these two methods were used to project the possible climate change impacts for the nine selected catchments of this study. More detailed descriptions of these two methods can be found in Luo et al. (2018b), Teutschbein and Seibert (2012) and Chen et al. (2013b).

3.2.1. EQM method of precipitation correction

The EQM method was applied point-wise, and empirical cumulative distribution functions (*ecdfs*) were constructed on a daily time-step to generate possible distribution of climate variables (Vrac and Friederichs, 2015). The EQM method produces possible *ecdfs* for both wet and dry days of precipitation time series. The average values, standard deviations, and the frequency of precipitation occurrence are corrected effectively in the EQM correction approach (Vormoor et al., 2015). The corrected precipitation can be expressed as follows:

$$P^{cor}_{HST,m,d} = ecdf^{-1}_{OBS,m}\left(ecdf_{HST,m}\left(P_{HST,m,d}\right)\right) \quad (3)$$

$$P^{cor}_{RCP,m,d} = ecdf^{-1}_{OBS,m}\left(ecdf_{HST,m}\left(P_{RCP,m,d}\right)\right) \quad (4)$$

where $P_{HST,\,m,\,d}$ and $P^{cor}_{HST,\,m,\,d}$ denote the precipitation before and after correction, respectively, in the historical period, while $P_{RCP,\,m,\,d}$ and $P^{cor}_{RCP,\,m,\,d}$ denote the precipitation before and after correction, respectively, in the future period under different emission scenarios. The subscripts *m* and *d* are the specific month and day, respectively. $ecdf^{-1}$ represents the inverse of *ecdf*.

3.2.2. Variance scaling (VARI) of temperature correction

VARI is an effective method to adjust both the average value and variance of temperature series (Teutschbein and Seibert, 2012). The corrected temperature can be calculated using Eqs. (5) and (6).

$$T^{cor}_{HST,m,d} = \left[T_{hst,m,d} - \mu\left(T_{hst,m}\right)\right] * \frac{\sigma_m\left(T_{OBS,m,d}\right)}{\sigma_m\left(T_{HST,m,d}\right)} \quad (5)$$

$$T^{cor}_{RCP,m,d} = \left[T_{RCP,m,d} - \mu\left(T_{RCP,m}\right)\right] * \frac{\sigma_m\left(T_{OBS,m,d}\right)}{\sigma_m\left(T_{HST,m,d}\right)} \quad (6)$$

where $T_{HST,\,m,\,d}$ and $T_{RCP,\,m,\,d}$ denote the temperature in the historical and future periods, respectively, while $T^{cor}_{HST,\,m,\,d}$ and $T^{cor}_{RCP,\,m,\,d}$ represent the corrected temperature in historical and future periods, respectively. $\mu(\cdot)$ and $\sigma(\cdot)$ represent the average value and standard deviation, respectively.

3.3. SWAT modelling using RCM predictions

To analyze the impact of future climate change on water resources, the most straightforward approach is to run future climate data in a hydrological model to obtain the climate-changed hydrological results (Steele-Dunne et al., 2008). In this study, the effects of climate change on river discharges were estimated by investigating the differences

between future (2021–2060) and historical time series (1965–2004) after correction. The climate change signals were further added to the driving climate series of the SWAT model to predict hydrological processes under the future emission scenarios. The newly generated precipitation and temperature are described by Eqs. (7) and (8), respectively.

$$P^{SWAT}_{RCP,m,d} = P^{SWAT}_{OBS,m,d} \times \frac{P^{cor}_{RCP,m,d}}{P^{cor}_{HST,m,d}} \quad (7)$$

$$T^{SWAT}_{RCP,m,d} = T^{SWAT}_{OBS,m,d} + \left(T^{cor}_{RCP,m,d} - T^{cor}_{HST,m,d}\right) \quad (8)$$

where $P^{SWAT}_{OBS,\,m,\,d}$ and $T^{SWAT}_{OBS,\,m,\,d}$ represent the observed precipitation and temperature, respectively applied to drive the SWAT model. $P^{SWAT}_{RCP,\,m,\,d}$ and $T^{SWAT}_{RCP,\,m,\,d}$ are the precipitation and temperature, respectively, with future climate change signals, which would be used to further calculate the relative changes in hydrological processes.

3.4. Sensitivity analysis

The sensitivity of water resources to climate change presents the response level of a specific hydrological component to the changes in a given climate variable or an emission scenario (Watson et al., 1996). In our study, the hydrological components, such as discharge, evapotranspiration and snow melting, have been considered and can be expressed as follows:

$$S = \frac{H_{\Delta+RAW} - H_{RAW}}{C_{\Delta+RAW} - C_{RAW}} \quad (9)$$

where H_{RAW} and C_{RAW} are the values of a hydrological component and climate variable, respectively, in the current period; $C_{\Delta+RAW}$ represents the value of a changed climate variable under a certain emission scenario, while $H_{\Delta+RAW}$ is the corresponding value of the hydrological component. Higher S means larger sensitivity of the hydrological component to the variation of a climate parameter. After sensitivity analysis, the importance of each climate variable in water resource changes can be understood (Lan et al., 2011).

4. Results

4.1. Hydrological modelling

The SWAT-simulated discharges correspond well with the observations for calibration and validation periods with both peak and low flows being captured well. The R^2 values ranged between 0.83 and 0.94 for the calibration period and between 0.77 and 0.94 for the validation period across all nine catchments (Table 2). The NSE values ranged between 0.67 and 0.92 for the calibration period and between 0.61 and 0.83 for the validation period. The satisfactory evaluation indices reflected the good performance of the SWAT model in simulating hydrological processes in these catchments.

Table 2
Statistics used to evaluate the SWAT model performances for the nine selected river catchments based on observed daily discharges.

	Calibration		Validation	
	R^2	NSE	R^2	NSE
HB(ALT)	0.93	0.92	0.80	0.61
BEJ(ALT)	0.90	0.87	0.89	0.62
YEQ(KKM)	0.84	0.69	0.87	0.69
HT(KKM)	0.83	0.68	0.87	0.77
SKS(NTSH)	0.91	0.81	0.89	0.77
ST(NTSH)	0.94	0.89	0.87	0.69
BY(NTSH)	0.90	0.87	0.77	0.63
TL(STSH)	0.86	0.72	0.94	0.83
KC(STSH)	0.86	0.67	0.83	0.68

4.2. The comparison of bias corrected results for precipitation and temperature

The performances of the three RCMs both before and after bias correction are presented in Fig. 3. The HadGEM3-RA outputs are significantly better than those of the other two models before correction. After bias correction, however, the three models showed similar performances in precipitation and temperature projections compared with observations, with correlation coefficients and amplitude of standard deviations being close to 1, and root-mean-square errors being <0.5. Furthermore, the ensemble results of the three RCMs were also compared. The mean absolute error between different models and ensemble results were <4.68% and 2.59% for precipitation and temperature, respectively. The results indicate the appropriateness of the selected bias correction methods. Considering the possible uncertainty of a single model, the climate change signals being calculated by ensemble results of the three models are used to further analyze the climate change impacts.

4.3. Precipitation and temperature trends for 2021–2060

The seasonal and annual precipitation changes under RCP 4.5 and RCP 8.5 based on the EQM method are shown in Fig. 4. The vertical bars represent the range of the changes calculated by different RCMs. In general, the three models presented similar changes in different catchments; therefore, the results will not be explained further. The annual precipitation continuously increases in the nine selected catchments, with higher increases always occurring under the RCP 8.5 scenario. The annual average increases in precipitation of the nine selected catchments are 6.45% (1.36–10.89%) and 9.28% (7.01–11.13%) under RCP 4.5 and RCP 8.5, respectively. The changes in spring (March–May, MAM), summer (June–August, JJA), autumn (September–November, SON) and winter (December–February of the next year, DJF) show large differences. In general, an increasing trend occurs in spring, autumn and winter, with the exception of the HT Catchment under the RCP 4.5 scenario. An obviously higher increasing ratio occurred in winter compared with other two seasons. In summer, the changing situation became more complex, and the three mountains presented different trends under the two scenarios as well. The precipitation showed a decreasing trend for both catchments in the ALT Mountains under RCP 4.5. Respective increasing and decreasing trends in summer precipitation were simulated for the YEQ and HT Catchments in the KKM Mountains under RCP 4.5. In the TSH Mountains, an increasing trend occurred for the KC and ST Catchments, while a decreasing trend was observed in the SKS, BY and TL Catchments under RCP 4.5. The catchments in ALT Mountains showed a clear decreasing trend in summer precipitation under RCP 8.5. However, an increasing trend occurred in summer precipitation for the catchments located in the KKM and TSH Mountains (but not the BY and HT Catchments) under RCP 8.5. These results indicate that the precipitation changes have spatial and temporal heterogeneity, especially in summer with diverse sensitivities for different scenarios.

VARI-corrected projections for all nine selected catchments exhibit a significant warming rate for both annual and seasonal temperatures (Figs. 5 and 6). The average annual maximum temperature will increase by 1.90 °C (1.76–2.02 °C) and 2.33 °C (2.25–2.48 °C) under RCP 4.5 and RCP 8.5 scenarios, respectively. The minimum temperature rises more than the maximum temperature, with average increasing values of 2.02 °C (1.77–2.20 °C) under RCP 4.5 and 2.45 °C (2.36–2.62 °C) under RCP 8.5 across all nine catchments. The result indicates that the diurnal temperature range (DTR) will narrow in the near future in this region. The temperature increases for catchments in the ALT and KKM Mountains are more pronounced than those in the NTSH and STSH

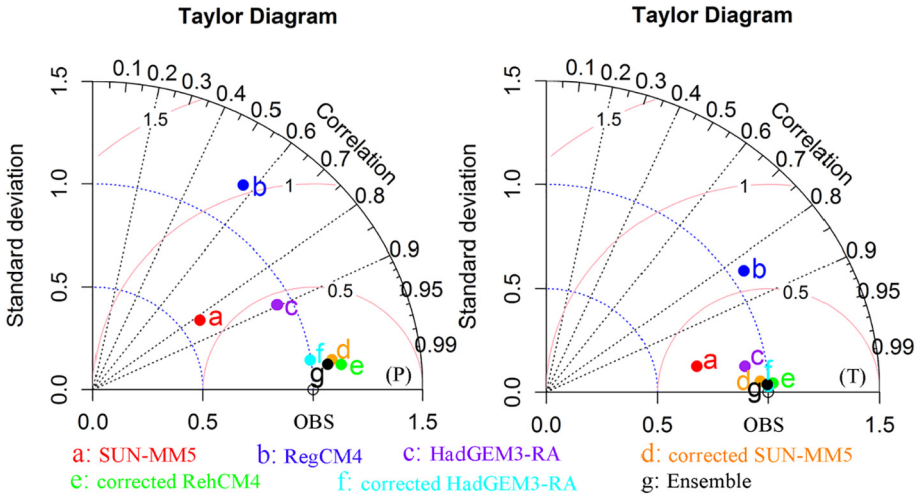

Fig. 3. The performance of each RCM and the bias correction results for precipitation and temperature during 1965–2004 (P: precipitation; T: temperature).

Mountains. Furthermore, different seasons will experience similar warming rankings. Except for the YEQ Catchment, the summer season is expected to experience the largest warming (2.20–2.54 °C) in maximum temperature under RCP 4.5 and RCP 8.5, followed by autumn (2.07–2.36 °C). For the minimum temperature, the most striking warming will occur in winter (2.18–2.59 °C). These results show that warming will mainly occur during the daytime in summer and during the night in winter. For the YEQ Catchment, the highest warming will occur in autumn for both maximum and minimum temperatures.

4.4. Simulated hydrological response under climate change scenarios

Fig. 7 shows the results of the annual and seasonal discharges across the nine catchments. These results show the combined effects of the changes in precipitation and temperature under different future emission scenarios. Climate change will increase the annual total discharge in the nine selected catchments. The average increasing values are 15.46% (0.37–41.04%) under RCP 4.5 and 18.85% (0.62–50.09%) under RCP 8.5 across all nine selected catchments. In general, the catchments in the ALT Mountains will have a relatively smaller change in annual discharge, with average values ranging between 0.79% and 4.46% under the two scenarios. In contrast, the catchments located in the KKM Mountains will present a discharge increase at a rate of 20.33–24.01%. The catchments located on the northern and southern slopes of the TSH Mountains will also experience obvious changes in annual discharge. The catchments in the NTSH Mountains will have a sharp change in discharge (28.00–31.90%) compared with catchments in STSH Mountains (6.48–8.51%). When focusing on the discharge changes in different seasons, all the catchments will experience strong positive changes in discharge during the spring season (10.60–99.66%

Fig. 4. The projected precipitation change for the period 2021–2060 under RCP 4.5 and RCP 8.5 scenarios compared with the historical period (1965–2004). The vertical bars represent the range of the changes calculated by different RCMs.

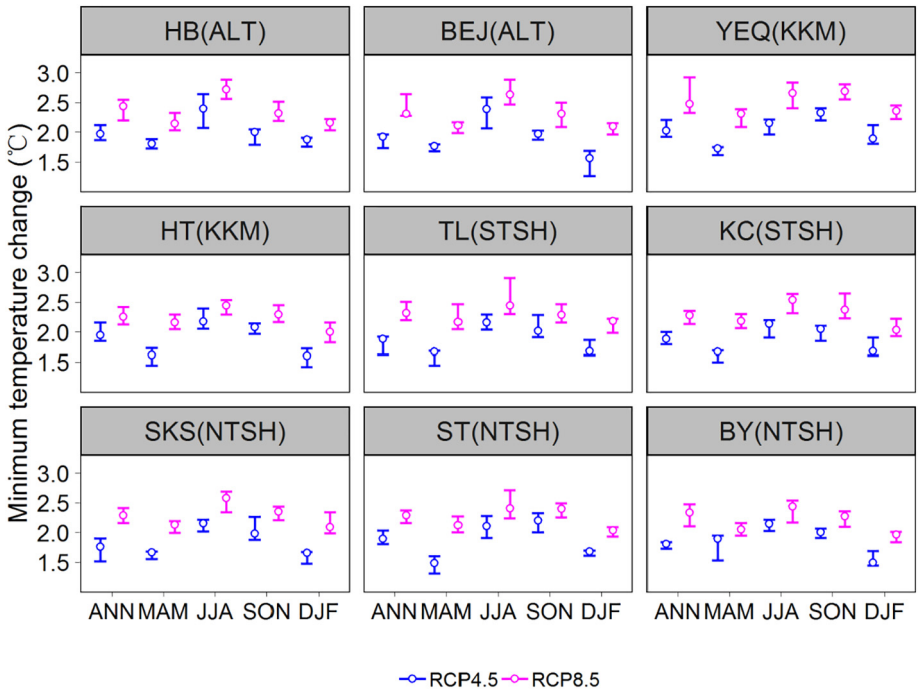

Fig. 5. The projected maximum temperature change for the period 2021–2060 under RCP 4.5 and RCP 8.5 scenarios compared to the historical period (1965–2004). The vertical bars represent the range of the changes calculated by different RCMs.

under RCP 4.5, 12.46–133.84% under RCP 8.5). We attribute the acute changes in spring to two reasons. Firstly, there is more snow accumulation in winter and the increased temperature will lead to more snowmelt water that supplies river discharge. Secondly, there will be more rainfall in spring, which will feed river discharge directly. However, the situation becomes more complicated in the other seasons. The HB Catchment in the ALT Mountains presents a decreasing trend in summer, autumn and winter discharges, while the BEJ Catchment exhibits a decreasing trend in summer discharge and an increasing trend in autumn and winter discharges. Except for winter discharge in HT, positive impacts are observed for the YEQ and HT Catchments in the KKM Mountains in terms of discharge in the three seasons. In STSH, the discharge in the TL Catchment exhibits a decreasing trend in summer and winter, while it presents an increasing trend in autumn. However, in the KC Catchment, the discharge in these three seasons will increase, with only a slight decrease (−2.04%) in winter under RCP 4.5. In the NTSH, the discharge in the SKS and ST Catchments will increase in different seasons, while a decreasing trend will occur in the BY Catchment

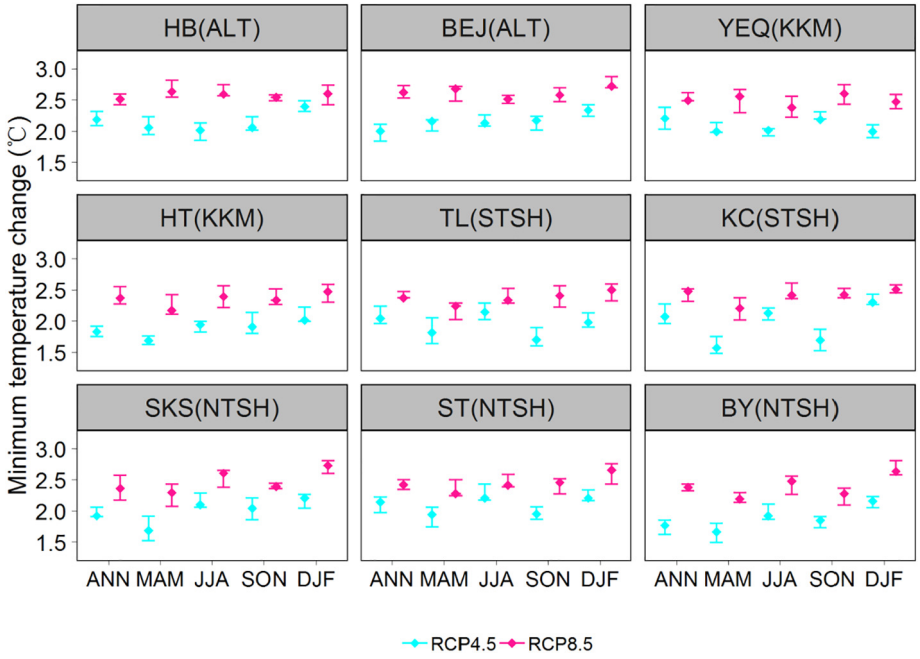

Fig. 6. The projected minimum temperature change for the period 2021–2060 under RCP 4.5 and RCP 8.5 scenarios, when compared with the historical period (1965–2004). The vertical bars represent the range of the changes calculated by different RCMs.

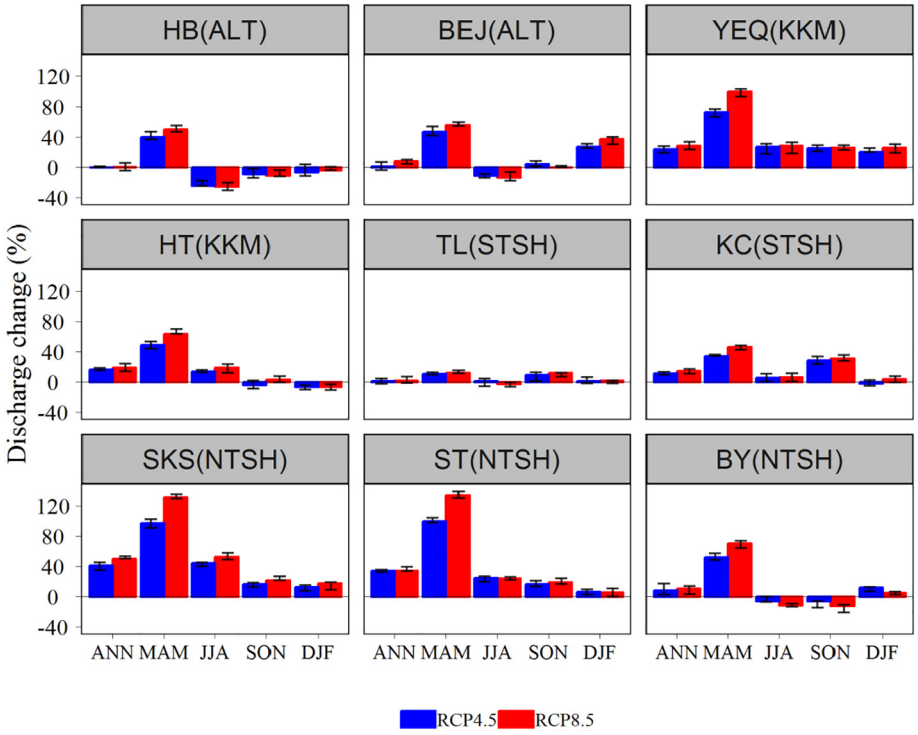

Fig. 7. The projected discharge change in the nine selected catchments for the period 2021–2060 under RCP 4.5 and RCP 8.5 scenarios compared to the historical period (1965–2004). The vertical bars represent the range of the changes calculated by different RCMs.

during the summer and autumn. Interestingly, for all the nine selected catchments, both the future emission scenarios yield a similar impact, but with different intensities.

The response of evapotranspiration to the projected climate change is shown in Fig. 8. In general, evapotranspiration presents an increasing trend at both annual and seasonal scales. The positive changes in evapotranspiration range between 8.56% and 22.67% for all nine selected catchments under RCP 4.5, with an average value of 14.58%. The increasing rates are even more pronounced under RCP 8.5, with an average value of 18.37% (11.49–24.37%). No obvious patterns can be attached in the change rates for different seasons. Since precipitation decreases will occur in some catchments during summer, the dual impacts of changes in precipitation and evapotranspiration are likely to cause a drier condition during summer in some regions.

Since the melting of snow is an important water resource in Xinjiang, the ice-snow melt water (Fig. 9) and the changes in ice-

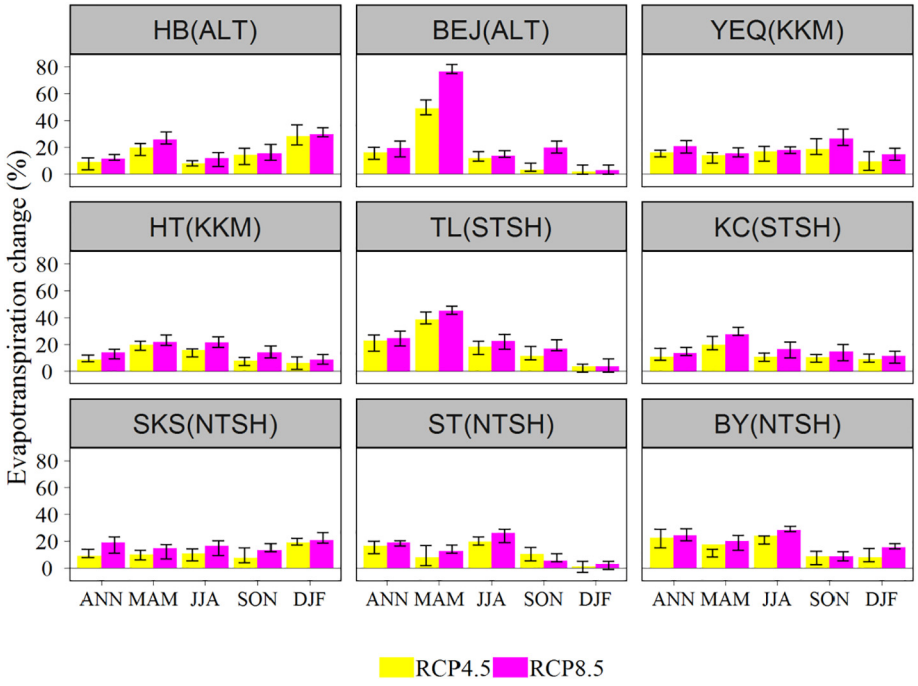

Fig. 8. The projected evapotranspiration change in the nine selected catchments for the period 2021–2060 under RCP 4.5 and RCP 8.5 scenarios compared with the historical period (1965–2004). The vertical bars represent the range of the changes calculated by different RCMs.

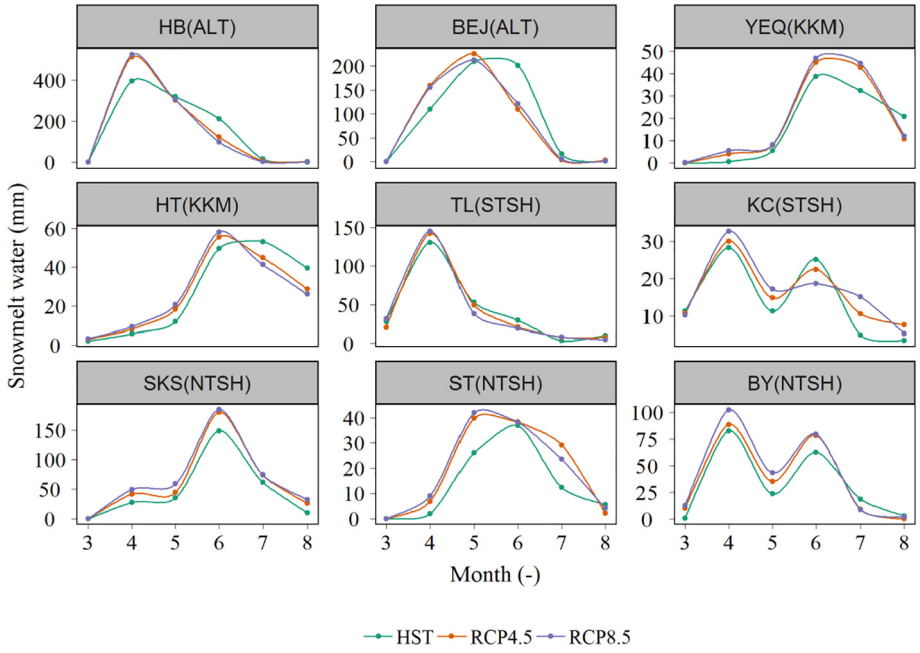

Fig. 9. The average snow melt for the nine selected catchments under historical, RCP 4.5, and RCP 8.5 scenarios.

snow melting (Fig. 10) under different emission scenarios were also analyzed. Because ice-snow melting mainly occurs in spring and summer, only the ice-snow melt water from March to August is presented in Fig. 9. In general, the catchments will experience important increases in ice-snow melting before the ice-snow melting peak. The ice-snow melting peak changes were in 1.18–32.25%, 4.49–21.08%, 6.40–15.57% and 7.32–23.93% for rivers in the ALT, KKM, STSH and NTSH Mountains, respectively. Because of the differences in the elevation between the two catchments in the ALT Mountains, the peaks of the snowmelt water occur in April and May for HB and BEJ, respectively. Since the YEQ and HT Catchments in the KKM Mountains are located at a higher elevation than the other catchments, the ice-snow melting peaks occur much later in June. The discharge from ice-snow melt will decrease after June in HT. However, it will still increase in YEQ in July and will only decrease after July. In the TSH Mountains, the KC and BY Catchments have two melting peaks that occur in April and June, respectively. The snowmelt water decreases after the snow melting peaks in the TL, KC and BY Catchments as well (the second peaks for KC and BY Catchments). Furthermore, the snowmelt water for the SKS and ST Catchments in NTSH always increases during the entire snowmelt period. The melting peak in the ST Catchment in NTSH Mountains will also occur one month earlier.

In general, a positive impact was observed in ice-snow melting for these alpine catchments except for TL in the STSH Mountains. The

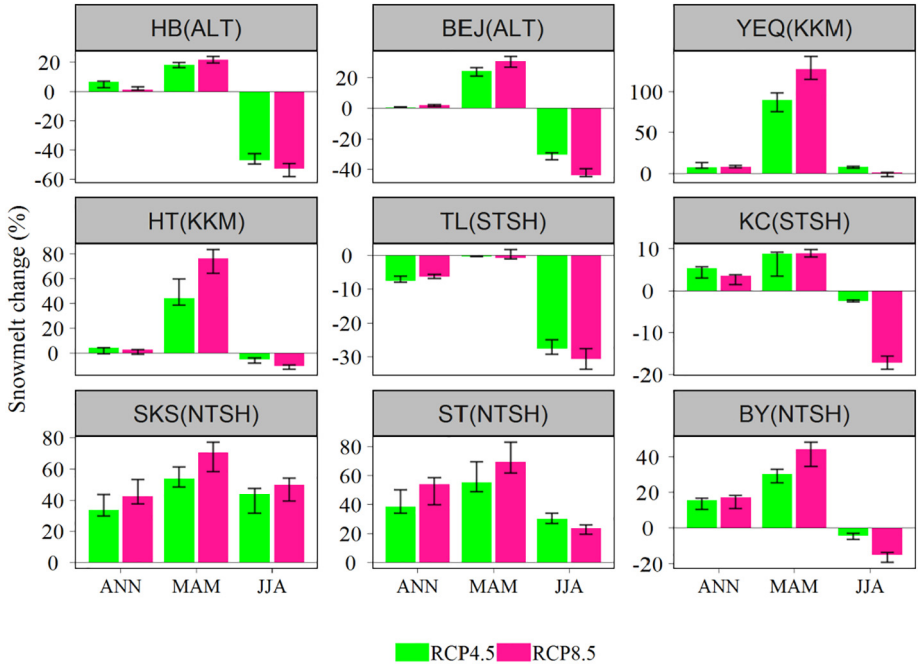

Fig. 10. The projected snow melting change in the nine selected catchments for the period 2021–2060 under RCP 4.5 and RCP 8.5 scenarios compared to the historical period (1965–2004). The vertical bars represent the range of the changes calculated by different RCMs.

annual predicted increases in snow melting water of the nine selected catchments were 11.59% (−7.61–38.49%) and 13.82% (−6.33–53.94%) under RCP 4.5 and RCP 8.5, respectively. The HB and BEJ Catchments in the ALT Mountains will have a relatively slower increasing ratio for ice-snow melting compared with the other catchments. When focusing on the seasonal fluctuations, positive and negative impacts are observed in spring and summer ice-snow melting, respectively, in the ALT Mountains. The same pattern was also observed for HT in the KKM Mountains, KC in the STSH Mountains, and BY in the NTSH Mountains. For YEQ in the KKM Mountains and SKS and ST in the NTSH Mountains, a positive impact was observed in both the spring and summer ice-snow melting. However, for the TL Catchment in STSH, snow melting always exhibited a decreasing trend, which can be attributed to the reduction in snowfall caused by warming.

4.5. The sensitivity of hydrological components to climate change

To evaluate the impact of changes in climatic variables on different hydrological components, the sensitivity of each hydrological component with respect to climate change was further investigated by driving the SWAT model with changes in precipitation and temperature separately. The sensitivity of discharge with respect to climate change is shown in Fig. 11. In general, the values of δD/δP ranged between 0.02 and 0.55 under RCP 4.5. The values show that when precipitation increased by 1%, the discharge increased by 0.02–0.55% across the nine selected catchments. However, the values became larger under RCP 8.5 in most regions, indicating the discharge is more sensitive under scenarios with larger precipitation changes. Furthermore, the discharge of catchments in northern Xinjiang was more sensitive to precipitation changes compared with those in southern Xinjiang. The sensitivities of discharge with respect to temperature changes are very different compared with precipitation. The values of δD/ΔT are less than zero (−2.24 to −0.56) for the HB and BEJ Catchments in the ALT Mountains, while they are larger than zero (0.20–17.31) for other catchments under RCP 4.5. The rising temperature will cripple the total discharge in the ALT Mountains, but it will multiply the total discharge for TSH and KKM Mountains under RCP 4.5. However, the values of sensitivities will decrease with a relative higher ΔT under RCP 8.5. The sensitivity value of the BY Catchment in the NTSH Mountains will become negative. This indicated that the increased discharge will level out or even tend to decrease with the consistently rising temperature since the larger ΔT undergoes lower increases or even decreases in total discharge. In addition, the discharge had higher sensitivity to rising temperature as compared with increasing precipitation.

The sensitivities of ice-snow melting and evapotranspiration in response to climate change are exhibited in Figs. 12 and 13, respectively. In general, the increases in precipitation and temperature will result in more snow melting for all nine selected catchments under RCP 4.5 in the study period. Snow melting is more vulnerable to temperature changes, with values ranging between 5.02 and 9.47. The values of sensitivity for precipitation ranged from 0.04 to 0.67 and from 0.28 to 1.23 under RCP 4.5 and RCP 8.5, respectively. The persistent rising temperature will not increase the ice-snow melting since the values of sensitivity will become negative in some catchments under RCP 8.5. Evapotranspiration is positively related to the increases in precipitation and temperature under both RCP 4.5 and RCP 8.5. The evapotranspiration presents greater sensitivity to the changes in temperature compared with those in precipitation.

4.6. The changes in the proportion of each hydrological component

In fact, for the alpine catchments in Xinjiang, the impact of climate change is more complicated because of the mixed ice-snow melt and rainfall regimes. The changes in supplies of discharge are shown in Fig. 14 based on the growing trend of warming and wetting for Xinjiang under RCP 4.5 and RCP 8.5 scenarios. The ratio of rainfall to discharge (R/D) for the HB and BEJ Catchments in the ALT Mountains exhibited an increasing trend. The same trend with greater percentages was also observed in the KKM Mountains. Interestingly, R/D for the catchments in the TSH Mountains presents diverse trend. An increasing trend of R/D was observed for the BY Catchment in NTSH and the TL and KC Catchments in STSH. A decreasing trend of R/D was observed for the SKS and ST Catchments in the NTSH Mountains. A lower ratio of S/P is observed across all nine selected catchments (Fig. 14). However, the proportion of evapotranspiration to precipitation (ET/P) indicated a positive impact for the nine selected catchments.

To better understand the different impact of the changes in precipitation and temperature, the separate impacts of each climatic variable on hydrological components were investigated as well (Table 3). The overall increasing precipitation crippled the rainfall percentages relative to total discharge. The changing values of R/D ranged between −2.12% and − 0.01%, with relatively higher absolute values observed in northern Xinjiang. Since the rising temperature impacts snowfall and ice-snow melting simultaneously, the impact of changing temperature is different in these catchments. Except for the SKS and ST Catchments in the NTSH Mountains, the rising temperature will increase the impact of rainfall on total discharge, especially in the catchments in the KKM Mountains with relatively higher elevation (>4 km). However, the rising temperature will weaken the R/D, with ΔR/D values ranging between −1.44% and −0.18% for the SKS and ST Catchments, respectively, in the NTSH Mountains.

For S/P and ET/P, the changing precipitation and temperature exhibit an adverse impact. The increases in precipitation contribute to the increases in S/P, with ΔS/P reaching 1.88%. In addition, they have a

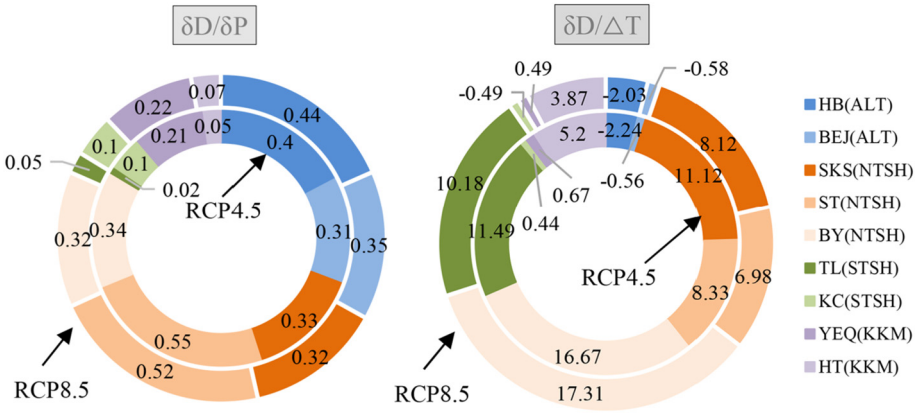

Fig. 11. The ratio of discharge change relative to precipitation (δD/δP) and temperature (δD/ΔT) for the 2021–2060 period under RCP 4.5 and RCP 8.5 scenarios compared to the historical period (1965–2004); δ and Δ represent the relative and absolute changes, respectively.

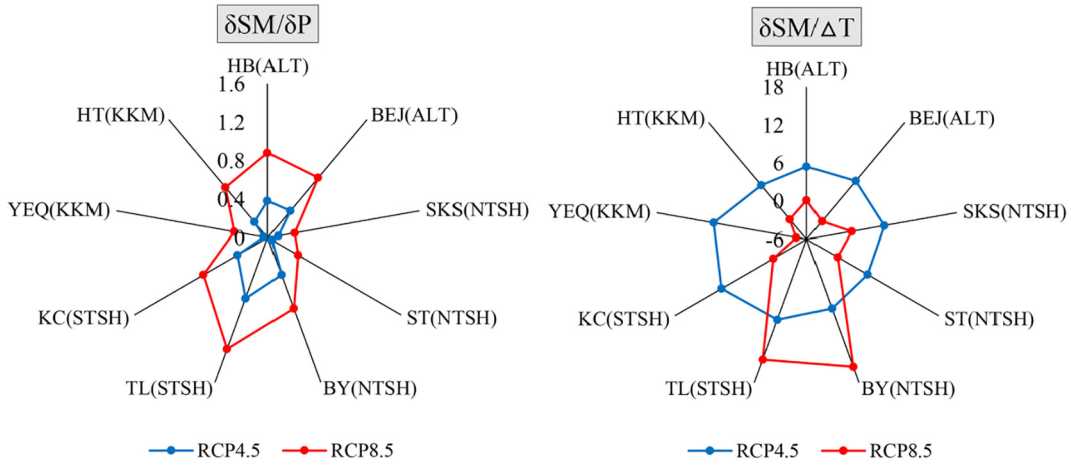

Fig. 12. The ratio of ice-snow melt change relative to precipitation (δSM/δP) and temperature (δSM/ΔT) for the 2021–2060 period under RCP 4.5 and RCP 8.5 scenarios compared with the historical period (1965–2004).

relatively greater impact on catchments in the ALT and NTSH Mountains (northern Xinjiang) than those in the KKM and STSH Mountains (southern Xinjiang). There is no doubt that the increasing temperature has a negative impact on S/P, with values ranging between −10.16% and −3.11% for the nine selected catchments. The changing precipitation and temperature exhibit a negative and positive impact, respectively, on ET/P. For the individual impact on ET/P, the precipitation increases are able to reduce the ET/P (−2.16–0%), while the increased temperature increases the ET/P (2.33–9.16%). The changing trends of these parameters are in line with the trends caused by temperature rising, which indicates a stronger impact from changes in temperature than from those in precipitation.

5. Discussion

5.1. Spatiotemporal characteristics of climate change

In the last few decades, research on the impact of climate change on water resources has increased. The main focus has been investigating the impact of climate change on catchments of a specific region. The regional similarities and differences of the impact of climate change caused by other factors of a catchment, such as location, elevation and area, have received much less attention (Lan et al., 2011).

Overall, the impact of climate change on the nine selected catchments in this study showed strong spatiotemporal heterogeneities. The climate is likely to become warmer and wetter in these catchments, while decreases in summer precipitation are likely for some catchments, especially in the ALT Mountains. Decreases in summer precipitation were also simulated in a previous study (Luo et al., 2018a). With increasing temperatures, the catchments in the ALT and KKM Mountains will warm faster, which can partly be explained by the differences in the latitude and elevation. According to previous studies, the temperature changes will become more pronounced at higher latitudes and elevations (Hu et al., 2014; Luo et al., 2019; Xue et al., 2003). The reason for the greater warming for catchments in the KKM Mountains compared with those in the TSH Mountains is attributed to the elevation differences. The average elevations of the two catchments in the KKM Mountains are distinctly higher (>4 km) than those of the catchments in the TSH Mountains, and the elevation dependence of warming is higher than the latitude dependence. The results further support the validity of the bias correction method used in this study. Furthermore, the increases in minimum temperature are more rapid than those for maximum temperature, which results in a decline in DTR. The result is generally in line with what is observed for most land areas around the world (Donat et al., 2013; Feng et al., 2018; Morak et al., 2013). Stronger variations in minimum temperature than in maximum temperature are likely to be attributed to the increasing vapor and aerosol content of the air (Wang et al., 2013). This reduces incoming solar radiation during the day as well as outgoing long wave radiation at night, causing a larger increase in the minimum temperature (Shen et al., 2010).

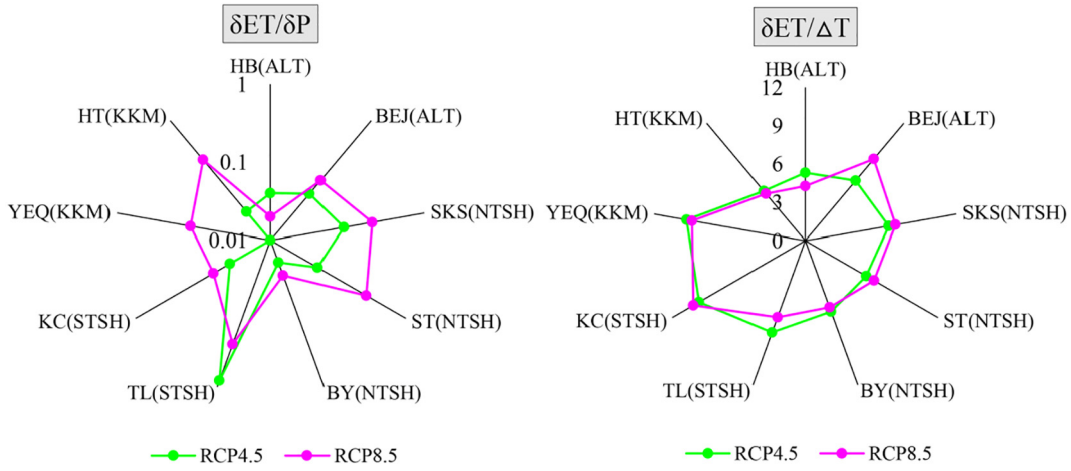

Fig. 13. The ratio of evapotranspiration change relative to precipitation (δET/δP) and temperature (δET/ΔT) for the 2021–2060 period under RCP 4.5 and RCP 8.5 scenarios compared to the historical period (1965–2004).

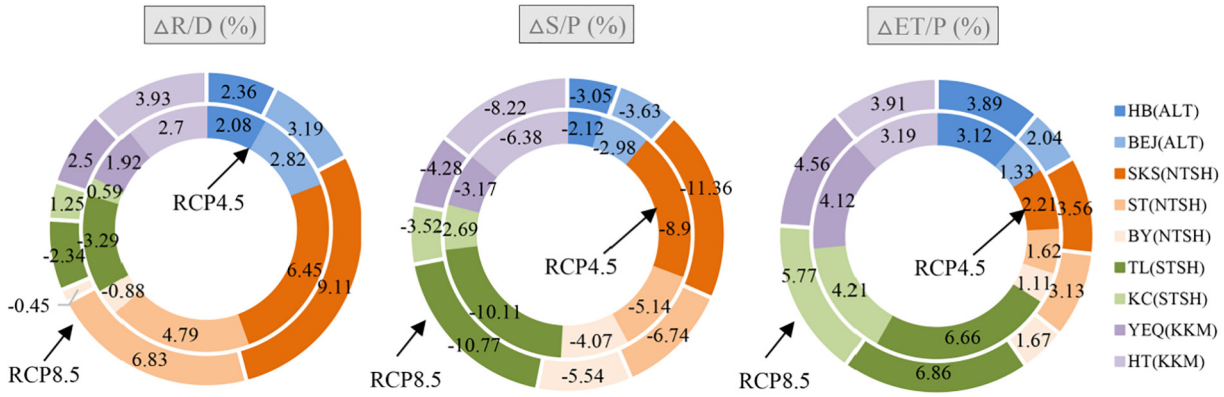

Fig. 14. The percentage changes in rainfall relative to discharge (ΔR/D), snowfall relative to precipitation (ΔS/P) and evapotranspiration relative to precipitation (ΔET/P) under RCP 4.5 and RCP 8.5 scenarios.

5.2. Variations in the impact of climate change caused by the differences in catchment characteristics

The impact of climate change on the total discharge is different across catchments. In general, the catchments located in the KKM and NTSH Mountains will have relatively larger increases in total discharge when compared with those in the ALT and STSH Mountains. The average changes in total discharge by the year of 2021–2060 are 0.79%, 20.33%, 28.00% and 6.48% for catchments in the ALT, KKM, NTSH and STSH Mountains, respectively, under the RCP 4.5 scenario. This can be attributed to the dependences of the impact on the location, area and elevation of the catchments. Larger catchments with higher elevation are more sensitive to climate change. For example, the BEJ Catchment presents greater average changes (1.22%) in discharge than the HB Catchment (0.37%) in the ALT Mountains. The changes in the YEQ Catchment are also higher than the changes in the HT Catchment in the KKM Mountains because of the differences in the elevation and area. Previous studies also indicated that high alpine catchments will experience the largest hydrological changes because of the important role of glacier and snow in the water balance (Beniston et al., 2003; Nijssen et al., 2001). However, the differences in the elevation and area do not completely account for the variations in the impact of climate change, such as the SKS and BY Catchments in NTSH Mountains and TL Catchment in the STSH Mountains. Lan et al. (2011) investigated the response of discharge to climate change in the Urumqi and Kaidu Catchments on the northern and southern slopes of the TSH Mountains. Different sensitivities were also observed for the two catchments with respect to the variations in precipitation and temperature. The results indicate that the slope aspect of the catchments also affects the responses of catchment to climate change. The northern slope of the TSH Mountains is the windward slope (Ji and Chen, 2012). The catchments on the windward slope of the TSH Mountains are more sensitive to climate change than the catchments on the leeward slope, likely because of the differences in water vapor sources, land cover, etc.

Table 3
The percentage changes in rainfall relative to discharge (ΔR/D), snowfall relative to precipitation (ΔS/P) and evapotranspiration relative to precipitation (ΔET/P) under separate precipitation changes (RCP4.5_P) and temperature changes scenarios (RCP4.5_T) from the RCP 4.5 scenario.

	ΔR/D (%)		ΔS/P (%)		ΔET/P (%)	
	RCP4.5_P	RCP4.5_T	RCP4.5_P	RCP4.5_T	RCP4.5_P	RCP4.5_T
HB (ALT)	−0.65	2.57	0.73	−3.11	−1.89	5.28
BEJ (ALT)	−0.71	3.14	0.82	−3.84	−1	2.46
YEQ (KKM)	−0.01	7.26	0.01	−9.33	−0.52	3.01
HT (KKM)	−0.17	5.38	0.32	−7.01	−0.05	2.33
SKS (NTSH)	−0.85	−0.18	0.56	−5.39	−0.98	2.52
ST (NTSH)	−2.12	−1.44	1.62	−10.16	−2.16	9.16
BY (NTSH)	−1.29	2.28	1.88	−4.37	−1.75	6.66
TL (STSH)	−0.11	1.81	0.2	−3.45	0	4.81
KC (STSH)	−0.52	3.77	0.37	−6.86	−0.37	3.27

5.3. Sensitivity transformation

This study demonstrates that all nine selected catchments experience increases in the total discharge under the RCP 4.5 and RCP 8.5 scenarios. The total discharge is more sensitive to the rising temperature than the increasing precipitation. This is easy to understand because for the high alpine catchments in Xinjiang, the temperature does not only affect the form of precipitation but also the volume of the snowmelt water (Liu et al., 2017). In fact, both increases in precipitation and temperature contribute to the increases in the total discharge, with the exception of temperature increases for the catchments in the ALT Mountains. Moreover, the total discharge in some catchments even exhibits sensitive transformation (from positive to negative) for higher increases in temperature under RCP 8.5. The same situation was also found in some other alpine catchments around the world, such as the Kaidu Catchment in Xinjiang (Fang et al., 2015b), the Zinal and Thur Catchments in Switzerland (Huss et al., 2008; Jasper et al., 2004) and the Athabasca Catchment in Canada (Shrestha et al., 2017). The results indicated that the increases in discharge are not sustainable in the study region. If the temperature continues to rise, the total discharge will be reduced in the future. Fang et al. (2015b) observed that the responses of discharge to temperature depended on the magnitude of the temperature increases in the Kaidu Catchment in Xinjiang. The discharge of the catchment will decrease when the temperature increases are higher than 2 °C. We concluded that there are critical temperatures for the sensitivity transformation in different catchments in Xinjiang. Increased temperatures might reach critical temperatures for the catchments in the ALT Mountains, even under the RCP 4.5 scenario. Therefore, the changes in temperature always show a negative impact on total discharge of the catchments in ALT Mountains.

5.4. Changes in different hydrological components

Even if the precipitation increases when the temperature does not change, the R/D still decreases, which is attributed to uneven variations in precipitation. Relatively larger increases in precipitation have been projected in winter when compared with summer, with decreases predicted in some catchments. Therefore, more precipitation will occur in the solid form under the precipitation change scenarios. The increased S/P under the same RCP4.5_P scenario further demonstrates this view. However, the impact of temperature increases is diverse for different catchments. The possible reasons are as follows. The increased temperature leads to greater water release from snow storage (Barnett et al.,

2005; Huss et al., 2008; Immerzeel et al., 2010), which increases the dependence of discharge on ice-snow melt water. In addition, the rising temperature results in more precipitation in liquid form. Therefore, when the rising temperature results in more snowmelt water than that transformed from snowfall to rainfall, the R/D ratio will increase under the temperature change scenarios; otherwise, an inverse situation will occur. In arid and semi-arid Xinjiang, the water resources will still increase in the near future. It is not difficult to imagine that the increase in the total discharge will not be sustained at the expense of the decreases in solid water storage. The catchments in arid and semi-arid regions in Xinjiang will more strongly depend on rainfall with decreases in S/P and solid water storage. These changes have a significant impact on water resource management and allocation, at both local and regional scales.

6. Conclusions

This study evaluated the impact of climate change under RCP 4.5 and RCP 8.5 emission scenarios on water resources in nine alpine catchments in arid and semi-arid Xinjiang. Although the total discharge of all nine selected catchments shows an overall increasing trend in the near future, the impact of climate change on different hydrological components indicated a strong spatiotemporal heterogeneity. The sensitivities of the impact of climate change are also highly dependent on the area, elevation and slope aspect of the catchments. The following conclusions can be drawn:

(1) The SWAT model performed well for hydrological modelling on both daily and monthly scales for the nine selected catchments, with R^2 and NSE values higher than 0.6.
(2) The annual precipitation experienced an overall increasing trend of 1.36–10.89% and 7.01–11.13% under RCP 4.5 and RCP 8.5, respectively, while summer precipitation decreased in some catchments, especially in the ALT Mountains. The trend of temperature changes depended on both latitude and elevation. The maximum temperature increased by 1.76–2.02 °C and by 2.25–2.48 °C under RCP 4.5 and RCP 8.5, respectively, with the summer season experiencing the strongest warming. The minimum temperature shows higher increases than maximum temperature, with increased values of 1.77–2.20 °C under RCP 4.5 and of 2.36–2.62 °C under RCP 8.5 across all nine selected catchments.
(3) The annual total river discharge showed increases in the range of 0.37–41.03% under RCP 4.5 and 0.62–50.09% under RCP 8.5 across the nine selected catchments with strong spatiotemporal heterogeneity. The most substantial increases in total discharge will occur in spring, while decreases in total discharge may occur in other seasons in some catchments. The catchments in the ALT and STSH Mountains are less sensitive to the impact of climate change compared with catchments located in the KKM and NTSH Mountains. The area, elevation and slope aspect of catchments will affect the intensities of the climate change impact.
(4) ET will increase in the near future with a range of 8.56–2.67% under RCP 4.5 and of 11.49–24.37% under RCP 8.5. Positive impacts of climate change will occur during snow melting in spring, while both positive and negative impacts will be expected for summer snow melting in different regions.
(5) Both δP and ΔT have a positive influence on the total discharge, while ΔT is associated with a higher sensitivity compared with δP. Northern Xinjiang shows a higher sensitivity to δP than southern Xinjiang. Each catchment has a critical temperature for the sensitivity transformation (from positive into negative) because of the continuous temperature rising.
(6) Finally, the proportion of each hydrologic component will also change significantly based on the results of this work. In general, the dependences of the total discharge on rainfall will increase with increased R/D. The S/P ratio presents a decreasing trend, while the ET/P ratio shows an increasing trend.

In general, increases in water resources in the near future are not sustainable since a large part of the increase is from the release of solid water storages. After some decades, depending on the characteristics of the catchment and climate change scenarios, the total discharge of these catchments in Xinjiang will drop below the current level. Therefore, the impact of climate change will have a large impact on water resource management and allocation. Decision makers should, therefore, formulate reasonable strategies according to the catchment characteristics to adapt to the impact of climate change.

Acknowledgements

This study was supported by the Strategic Priority Research Program of Chinese Academy of Sciences, Pan-Third Pole Environment Study for a Green Silk Road (Grant No. XDA20060303), the State's Key Project of Research and Development Plan (Grant No. 2017YFC0404501), the National Natural Science Foundation of China (Grant No.41761144079/U1503183), the International Partnership Program of the Chinese Academy of Sciences (Grant No. 131551KYSB20160002), and the Tianshan Innovation Team Project of the Xinjiang Department of Science and Technology (Grant No. Y744261).

Conflict of interests

The authors declare that there is no conflict of interests regarding the publication of this paper.

References

Abbaspour, K.C., Yang, J., Maximov, I., Siber, R., Bogner, K., Mieleitner, J., et al., 2007. Modelling hydrology and water quality in the pre-alpine/alpine Thur watershed using SWAT. J. Hydrol. 333, 413–430. https://doi.org/10.1016/j.jhydrol.2006.09.014.
Arnold, J.G., Srinivasan, R., Muttiah, R.S., Williams, J.R., 1998. Large area hydrologic modeling and assessment part I: model development 1. J. Am. Water Resour. Assoc. 34, 73–89. https://doi.org/10.1111/j.1752-1688.1998.tb05961.x.
Ba, W., Du, P., Liu, T., Bao, A., Luo, M., Hassan, M., et al., 2018. Simulating hydrological responses to climate change using dynamic and statistical downscaling methods: a case study in the Kaidu River Basin, Xinjiang, China. J. Arid. Land 10, 905–920. https://doi.org/10.1007/s40333-018-0068-0.
Baker, T.J., Miller, S.N., 2013. Using the Soil and Water Assessment Tool (SWAT) to assess land use impact on water resources in an East African watershed. J. Hydrol. 486, 100–111. https://doi.org/10.1016/j.jhydrol.2013.01.041.
Barnett, T.P., Adam, J.C., Lettenmaier, D.P., 2005. Potential impacts of a warming climate on water availability in snow-dominated regions. Nature 438, 303. https://doi.org/10.1038/nature04141.
Beniston, M., Keller, F., Goyette, S., 2003. Snow pack in the Swiss Alps under changing climatic conditions: an empirical approach for climate impacts studies. Theor. Appl. Climatol. 74, 19–31. https://doi.org/10.1007/s00704-002-0709-1.
Bradley, R.S., Vuille, M., Diaz, H.F., Vergara, W., 2006. Threats to water supplies in the tropical Andes. Science 312, 1755–1756. https://doi.org/10.1126/science.1128087.
Casanueva, A., Kotlarski, S., Herrera, S., Fernández, J., Gutiérrez, J.M., Boberg, F., et al., 2016. Daily precipitation statistics in a EURO-CORDEX RCM ensemble: added value of raw and bias-corrected high-resolution simulations. Clim. Dyn. 47, 719–737. https://doi.org/10.1007/s00382-015-2865-x.
Chen, J., Brissette, F.P., Poulin, A., Leconte, R., 2011. Overall uncertainty study of the hydrological impacts of climate change for a Canadian watershed. Water Resour. Res. 47. https://doi.org/10.1029/2011WR010602.
Chen, J., Brissette, F.P., Chaumont, D., Braun, M., 2013a. Finding appropriate bias correction methods in downscaling precipitation for hydrologic impact studies over North America. Water Resour. Res. 49, 4187–4205.
Chen, J., Brissette, F.P., Chaumont, D., Braun, M., 2013b. Performance and uncertainty evaluation of empirical downscaling methods in quantifying the climate change impacts on hydrology over two North American river basins. J. Hydrol. 479, 200–214.
Donat, M., Alexander, L., Yang, H., Durre, I., Vose, R., Dunn, R., et al., 2013. Updated analyses of temperature and precipitation extreme indices since the beginning of the twentieth century: the HadEX2 dataset. J. Geophys. Res.-Atmos. 118, 2098–2118. https://doi.org/10.1002/jgrd.50150.
Dosio, A., Panitz, H.-J., Schubert-Frisius, M., Lüthi, D., 2015. Dynamical downscaling of CMIP5 global circulation models over CORDEX-Africa with COSMO-CLM: evaluation over the present climate and analysis of the added value. Clim. Dyn. 44, 2637–2661. https://doi.org/10.1007/s00382-014-2262-x.

Du, J., Shu, J., Yin, J., Yuan, X., Jiaerheng, A., Xiong, S., et al., 2015. Analysis on spatio-temporal trends and drivers in vegetation growth during recent decades in Xinjiang, China. Int. J. Appl. Earth Obs. Geoinf. 38, 216–228. https://doi.org/10.1016/j.jag.2015.01.006.

Durman, C., Gregory, J.M., Hassell, D.C., Jones, R., Murphy, J., 2001. A comparison of extreme European daily precipitation simulated by a global and a regional climate model for present and future climates. Q. J. R. Meteorol. Soc. 127, 1005–1015.

Fang, G., Yang, J., Chen, Y., Zammit, C., 2015a. Comparing bias correction methods in downscaling meteorological variables for a hydrologic impact study in an arid area in China. Hydrol. Earth Syst. Sci. 19, 2547–2559.

Fang, G., Yang, J., Chen, Y., Zhang, S., Deng, H., Liu, H., et al., 2015b. Climate change impact on the hydrology of a typical watershed in the Tianshan Mountains. Adv. Meteorol. 2015, 1–10.

Feng, R., Yu, R., Zheng, H., Gan, M., 2018. Spatial and temporal variations in extreme temperature in Central Asia. Int. J. Climatol. 38, e388–e400. https://doi.org/10.1002/joc.5379.

Fowler, H.J., Blenkinsop, S., Tebaldi, C., 2007. Linking climate change modelling to impacts studies: recent advances in downscaling techniques for hydrological modelling. Int. J. Climatol. 27, 1547–1578. https://doi.org/10.1002/joc.1556.

Giorgi, F., Gutowski Jr., W.J., 2015. Regional dynamical downscaling and the CORDEX initiative. Annu. Rev. Environ. Resour. 40, 467–490. https://doi.org/10.1146/annurev-environ-102014-021217.

Grusson, Y., Sun, X., Gascoin, S., Sauvage, S., Raghavan, S., Anctil, F., et al., 2015. Assessing the capability of the SWAT model to simulate snow, snow melt and streamflow dynamics over an alpine watershed. J. Hydrol. 531, 574–588. https://doi.org/10.1016/j.jhydrol.2015.10.070.

Hu, Z., Zhang, C., Hu, Q., Tian, H., 2014. Temperature changes in Central Asia from 1979 to 2011 based on multiple datasets. J. Clim. 27, 1143–1167. https://doi.org/10.1175/JCLI-D-13-00064.1.

Hundecha, Y., Sunyer, M.A., Lawrence, D., Madsen, H., Willems, P., Bürger, G., et al., 2016. Inter-comparison of statistical downscaling methods for projection of extreme flow indices across Europe. J. Hydrol. 541, 1273–1286. https://doi.org/10.1016/j.jhydrol.2016.08.033.

Huss, M., Farinotti, D., Bauder, A., Funk, M., 2008. Modelling runoff from highly glacierized alpine drainage basins in a changing climate. Hydrol. Process. 22, 3888–3902. https://doi.org/10.1002/hyp.7055.

Immerzeel, W.W., Van Beek, L.P., Bierkens, M.F., 2010. Climate change will affect the Asian water towers. Science 328, 1382–1385. https://doi.org/10.1126/science.1183188.

Jacob, D., Petersen, J., Eggert, B., Alias, A., Christensen, O.B., Bouwer, L.M., et al., 2014. EURO-CORDEX: new high-resolution climate change projections for European impact research. Reg. Environ. Chang. 14, 563–578. https://doi.org/10.1007/s10113-013-0499-2.

Jasper, K., Calanca, P., Gyalistras, D., Fuhrer, J., 2004. Differential impacts of climate change on the hydrology of two alpine river basins. Clim. Res. 26, 113–129. https://doi.org/10.3354/cr026113.

Ji, X., Chen, Y., 2012. Characterizing spatial patterns of precipitation based on corrected TRMM 3 B 43 data over the mid Tianshan Mountains of China. J. Mt. Sci. 9, 628–645. https://doi.org/10.1007/s11629-012-2283-z.

Lan, Y., Zhong, Y., Wu, S., Shen, Y., Wang, G., La, C., et al., 2011. Response of mountain runoff to climate change in representative rivers originated from the Tianshan Mountain. J. Desert Res. 31, 254–260.

Lespinas, F., Ludwig, W., Heussner, S., 2014. Hydrological and climatic uncertainties associated with modeling the impact of climate change on water resources of small Mediterranean coastal rivers. J. Hydrol. 511, 403–422. https://doi.org/10.1016/j.jhydrol.2014.01.033.

Li, X., Jiang, F., Li, L., Wang, G., 2011. Spatial and temporal variability of precipitation concentration index, concentration degree and concentration period in Xinjiang, China. Int. J. Climatol. 31, 1679–1693.

Liu, T., Willems, P., Pan, X., Bao, A.M., Chen, X., Veroustraete, F., et al., 2011. Climate change impact on water resource extremes in a headwater region of the Tarim basin in China. Hydrol. Earth Syst. Sci. 15, 6593–6637.

Liu, J., Liu, T., Bao, A., De Maeyer, P., Feng, X., Miller, S.N., et al., 2016. Assessment of different modelling studies on the spatial hydrological processes in an arid alpine catchment. Water Resour. Manag. 30, 1757–1770. https://doi.org/10.1007/s11269-016-1249-2.

Liu, J., Luo, M., Liu, T., Bao, A., De Maeyer, P., Feng, X., et al., 2017. Local climate change and the impacts on hydrological processes in an arid alpine catchment in Karakoram. Water 9, 344. https://doi.org/10.3390/w9050344.

Luo, M., Meng, F., Liu, T., Duan, Y., Frankl, A., Kurban, A., et al., 2017. Multi–model ensemble approaches to assessment of effects of local climate change on water resources of the Hotan River Basin in Xinjiang, China. Water 9, 584. https://doi.org/10.3390/w9080584.

Luo, M., Liu, T., Frankl, A., Duan, Y., Meng, F., Bao, A., et al., 2018a. Defining spatiotemporal characteristics of climate change trends from downscaled GCMs ensembles: how climate change reacts in Xinjiang, China. Int. J. Climatol. 38, 2538–2553.

Luo, M., Liu, T., Meng, F., Duan, Y., Frankl, A., Bao, A., et al., 2018b. Comparing bias correction methods used in downscaling precipitation and temperature from regional climate models: a case study from the Kaidu River Basin in Western China. Water 10, 1046.

Luo, M., Liu, T., Meng, F., Duan, Y., Bao, A., Frankl, A., et al., 2019. Spatiotemporal characteristics of future changes in precipitation and temperature in Central Asia. Int. J. Climatol. 39, 1571–1588. https://doi.org/10.1002/joc.5901.

Morak, S., Hegerl, G.C., Christidis, N., 2013. Detectable changes in the frequency of temperature extremes. J. Clim. 26, 1561–1574. https://doi.org/10.1175/JCLI-D-11-00678.1.

Nijssen, B., O'donnell, G.M., Hamlet, A.F., Lettenmaier, D.P., 2001. Hydrologic sensitivity of global rivers to climate change. Clim. Chang. 50, 143–175. https://doi.org/10.1023/A:1010616428763.

Piani, C., Haerter, J., Coppola, E., 2010. Statistical bias correction for daily precipitation in regional climate models over Europe. Theor. Appl. Climatol. 99, 187–192. https://doi.org/10.1007/s00704-009-0134-9.

Pinto, I., Jack, C., Hewitson, B., 2018. Process-based model evaluation and projections over southern Africa from coordinated regional climate downscaling experiment and coupled model intercomparison project phase 5 models. Int. J. Climatol. 38, 4251–4261. https://doi.org/10.1002/joc.5666.

Shen, Y., Liu, C., Liu, M., Zeng, Y., Tian, C., 2010. Change in pan evaporation over the past 50 years in the arid region of China. Hydrol. Process. 24, 225–231.

Shrestha, N.K., Du, X., Wang, J., 2017. Assessing climate change impacts on fresh water resources of the Athabasca River Basin, Canada. Sci. Total Environ. 601, 425–440.

Steele-Dunne, S., Lynch, P., McGrath, R., Semmler, T., Wang, S., Hanafin, J., et al., 2008. The impacts of climate change on hydrology in Ireland. J. Hydrol. 356, 28–45. https://doi.org/10.1016/j.jhydrol.2008.03.025.

Sunyer, M.A., Hundecha, Y., Lawrence, D., Madsen, H., Willems, P., Martinkova, M., et al., 2015. Inter-comparison of statistical downscaling methods for projection of extreme precipitation in Europe. Hydrol. Earth Syst. Sci. 19, 1827–1847. https://doi.org/10.5194/hess-19-1827-2015.

Teutschbein, C., Seibert, J., 2012. Bias correction of regional climate model simulations for hydrological climate-change impact studies: review and evaluation of different methods. J. Hydrol. 456, 12–29.

Vormoor, K., Lawrence, D., Heistermann, M., Bronstert, A., 2015. Climate change impacts on the seasonality and generation processes of floods – projections and uncertainties for catchments with mixed snowmelt/rainfall regimes. Hydrol. Earth Syst. Sci. 19, 913–931. https://doi.org/10.5194/hess-19-913-2015.

Vrac, M., Friederichs, P., 2015. Multivariate—intervariable, spatial, and temporal—bias correction. J. Clim. 28, 218–237. https://doi.org/10.1175/JCLI-D-14-00059.1.

Wang, G.-x., Cheng, G.-d., 2000. The characteristics of water resources and the changes of the hydrological process and environment in the arid zone of northwest China. Environ. Geol. 39, 783–790. https://doi.org/10.1007/s002540050494.

Wang, H., Chen, Y., Xun, S., Lai, D., Fan, Y., Li, Z., 2013. Changes in daily climate extremes in the arid area of northwestern China. Theor. Appl. Climatol. 112, 15–28. https://doi.org/10.1007/s00704-012-0698-7.

Watson, R.T., Zinyowera, M.C., Moss, R.H., 1996. Climate Change 1995. Impacts, Adaptations and Mitigation of Climate Change: Scientific-Technical Analyses.

Wilby, R.L., Wigley, T., 1997. Downscaling general circulation model output: a review of methods and limitations. Prog. Phys. Geogr. 21, 530–548.

Xue, Y., Han, P., Feng, G., 2003. Change trend of the precipitation and air temperature in Xinjiang since recent 50 years. Arid Zone Res. 20, 127–130.

Yang, W., Andréasson, J., Phil Graham, L., Olsson, J., Rosberg, J., Wetterhall, F., 2010. Distribution-based scaling to improve usability of regional climate model projections for hydrological climate change impacts studies. Hydrol. Res. 41, 211–229. https://doi.org/10.2166/nh.2010.004.

Zhang, Q., Xu, C.-Y., Zhang, Z., Ren, G., Chen, Y., 2008. Climate change or variability? The case of Yellow river as indicated by extreme maximum and minimum air temperature during 1960–2004. Theor. Appl. Climatol. 93, 35–43. https://doi.org/10.1007/s00704-007-0328-y.

Zhang, Q., Sun, P., Li, J., Singh, V.P., Liu, J., 2015. Spatiotemporal properties of droughts and related impacts on agriculture in Xinjiang, China. Int. J. Climatol. 35, 1254–1266. https://doi.org/10.1002/joc.4052.

Zhang, Y., Luo, Y., Sun, L., 2016. Quantifying future changes in glacier melt and river runoff in the headwaters of the Urumqi River, China. Environ. Earth Sci. 75, 770.

Zou, L., Zhou, T., Peng, D., 2016. Dynamical downscaling of historical climate over CORDEX East Asia domain: a comparison of regional ocean-atmosphere coupled model to stand-alone RCM simulations. J. Geophys. Res.-Atmos. 121, 1442–1458. https://doi.org/10.1002/2015JD023912.